Article

Cell Reports

Lateral Preoptic Control of the Lateral Habenula through Convergent Glutamate and GABA Transmission

Graphical Abstract

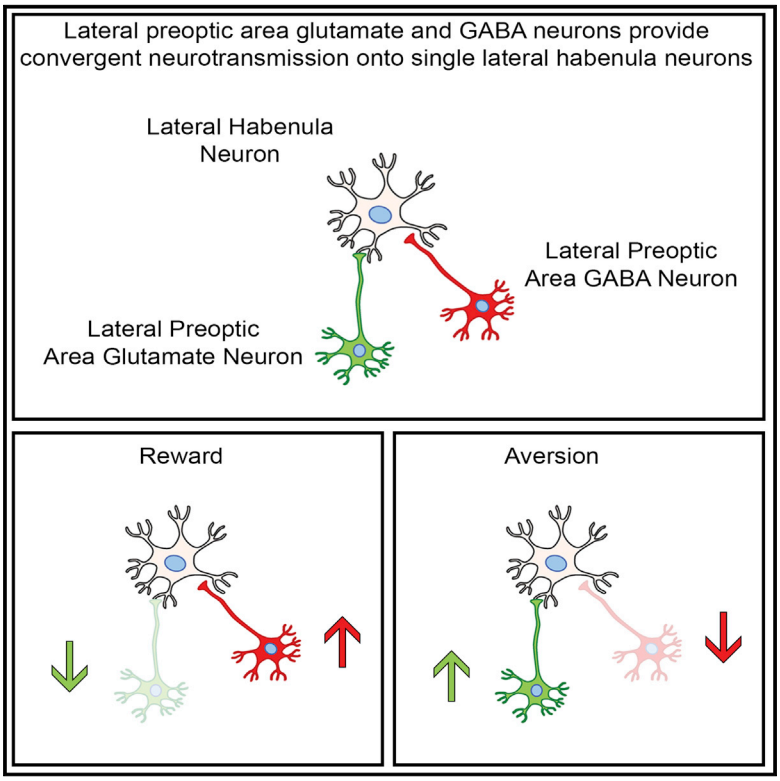

Authors

David J. Barker, Jorge Miranda-Barrientos, Shiliang Zhang, ..., Bing Liu, Erin S. Calipari, Marisela Morales

Correspondence

mmorales@intra.nida.nih.gov

In Brief

Barker et al. show that distinct populations of lateral preoptic area glutamate and GABA neurons synapse together on single lateral habenula neurons and find that this "convergent neurotransmission" allows preoptic area neurons to exert bivalent control over single lateral habenula neurons and drive opposing motivational states.

Highlights

- The LPO→LHb pathway is predominantly glutamatergic
- LPO glutamate and GABA provide convergent neurotransmission onto single LHb neurons
- Noxious stimuli activate both LPO→LHb glutamate and GABA concurrently
- Independent activation of glutamate or GABA drives opposing motivational states

Barker et al., 2017, Cell Reports *21*, 1757–1769
November 14, 2017
https://doi.org/10.1016/j.celrep.2017.10.066

Cell Reports
Article

OPEN ACCESS
CellPress

Lateral Preoptic Control of the Lateral Habenula through Convergent Glutamate and GABA Transmission

David J. Barker,[1,4] Jorge Miranda-Barrientos,[1,4] Shiliang Zhang,[2] David H. Root,[1] Hui-Ling Wang,[1] Bing Liu,[1] Erin S. Calipari,[3] and Marisela Morales[1,5,*]

[1]Neuronal Networks Section, Integrative Neuroscience Research Branch, National Institute on Drug Abuse, 251 Bayview Blvd., Suite 200, Baltimore, MD 21224, USA
[2]Electron Microscopy Core, National Institute on Drug Abuse, 251 Bayview Blvd., Suite 200, Baltimore, MD 21223, USA
[3]Fishberg Department of Neuroscience and Friedman Brain Institute, Icahn School of Medicine at Mount Sinai, New York, NY 10029, USA
[4]These authors contributed equally
[5]Lead Contact
*Correspondence: mmorales@intra.nida.nih.gov
https://doi.org/10.1016/j.celrep.2017.10.066

SUMMARY

The lateral habenula (LHb) is a brain structure that participates in cognitive and emotional processing and has been implicated in several mental disorders. Although one of the largest inputs to the LHb originates in the lateral preoptic area (LPO), little is known about how the LPO participates in the regulation of LHb function. Here, we provide evidence that the LPO exerts bivalent control over the LHb through the convergent transmission of LPO glutamate and γ-aminobutyric acid (GABA) onto single LHb neurons. *In vivo*, both LPO-glutamatergic and LPO-GABAergic inputs to the LHb are activated by aversive stimuli, and their predictive cues yet produce opposing behaviors when stimulated independently. These results support a model wherein the balanced response of converging LPO-glutamate and LPO-GABA are necessary for a normal response to noxious stimuli, and an imbalance in LPO→LHb glutamate or GABA results in the type of aberrant processing that may underlie mental disorders.

INTRODUCTION

The lateral habenula (LHb) is a brain structure that is involved in cognitive and emotional processing. LHb activity is regulated by inputs from the basal forebrain, prefrontal cortex, hypothalamus, and basal ganglia, and in turn, LHb outputs influence several systems, including the dopamine, serotonin, and noradrenaline systems (Namboodiri et al., 2016). It has been hypothesized that alterations of LHb activity play a role in mental disorders that involve aberrant monoaminergic signaling and affective processing, including depression and addiction (Aizawa et al., 2013; Jhou et al., 2013). Thus, to understand the role of the LHb in mental disorders, it is necessary to determine the types of neurons from different brain areas that establish synaptic connectivity with the LHb and how these different synaptic inputs influence LHb activity and different aspects of behavior.

The LHb is comprised of mostly glutamatergic neurons (Lecca et al., 2014), and currently, there is no evidence for the existence of LHb γ-aminobutyric-acid (GABA)-releasing neurons. Thus, our understanding of the LHb cellular composition suggests that inhibition of the LHb is accomplished through inhibitory, long-range inputs to the LHb. Recent studies have shown that major sources of GABAergic innervation to the LHb are from dual glutamatergic-GABAergic neurons that are distributed in both the ventral tegmental area (VTA) (Root et al., 2014b) and the entopeduncular nucleus (EPN) (Shabel et al., 2014). Furthermore, LHb immuno-ultrastructural analyses have demonstrated that the majority of axon terminals (≈53%) within the LHb have the capability to co-release glutamate and GABA as they co-express transporters for the vesicular accumulation of glutamate (vesicular glutamate transporter 2 [VGluT2]) or GABA (vesicular GABA transporter [VGAT]). However, these ultrastructural studies have also shown that a fraction of terminals within the LHb release only glutamate (≈33%) or GABA (≈13%) (Root et al., 2014b). While some of the inputs that release only glutamate or GABA originate in the VTA (Root et al., 2014a, 2014b) or lateral hypothalamus (LH) (Stamatakis et al., 2016), the origin of most of the glutamate- or GABA-only inputs innervating the LHb is unclear.

One of the largest inputs to the LHb originates from the lateral preoptic area (LPO) (Yetnikoff et al., 2015), and anatomical and electrophysiological findings from over forty years of research have led to the suggestion that LPO→LHb inputs are GABAergic (Araki et al., 1984; Garland and Mogenson, 1983; Heimer and Alheid, 1991; Meye et al., 2013; Mok and Mogenson, 1972a, 1972b). Nevertheless, the cellular composition and behavioral function of LPO→LHb inputs and their influence on LHb mediated behaviors are unclear. In the present study, we used a multidisciplinary approach to characterize the phenotype and synaptic properties of LPO→LHb inputs, observe the dynamic properties of these inputs during motivated behavior, and causally manipulate these inputs to determine their motivational valence. In contrast to the prevailing idea that the LPO→LHb pathway is GABAergic, we found that most of the LPO neurons innervating the LHb are glutamatergic and that only a small subset are GABAergic. Nonetheless, by ultrastructural and electrophysiological approaches, we found an

This is an open access article under the CC BY-NC-ND license (http://creativecommons.org/licenses/by-nc-nd/4.0/).

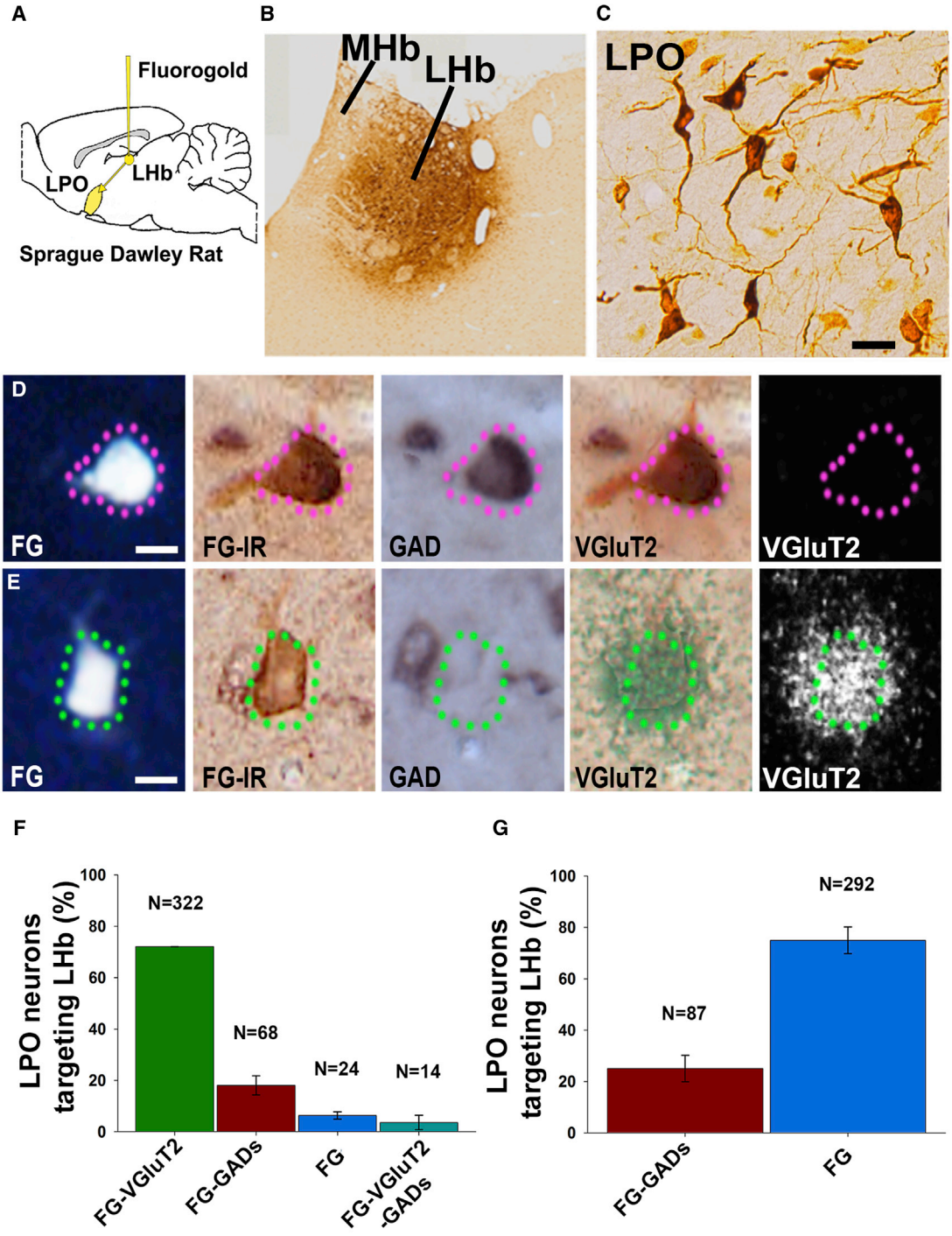

Figure 1. Major Input from the Lateral Preoptic Area to the Lateral Habenula Is from Glutamatergic Neurons

(A) Iontophoretic delivery of the retrograde tract tracer Fluorogold (FG) into the LHb.

(B and C) FG injection site in the LHb (B) and retrogradely labeled LPO→LHb neurons (C).

(D and E) Phenotypic characterization of LPO→LHb neurons. FG is seen as white or brown after its immunodetection (FG-immunoreactivity [IR]). (D) LPO→LHb neuron expressing GADs mRNA (detection with non-radioactive probe; purple cell). (E) LPO→LHb neuron expressing VGluT2 mRNA (detection with radioactive probe; cell with green or silver grains).

(legend continued on next page)

unexpected type of neurotransmission by which independent populations of LPO-glutamatergic neurons and LPO-GABAergic neurons provide convergent neurotransmission onto single LHb neurons. Convergent LPO-glutamatergic and LPO-GABAergic inputs to LHb are simultaneously activated during aversive conditioning, suggesting that the LPO influence on LHb during aversion is by the co-reception of glutamate and GABA. By isolating the LPO-LHb glutamatergic or LPO-LHb pathways with optogenetics, we found that the independent activation of LPO→LHb glutamate neurons results in aversion, while the activation of LPO→LHb GABA results in reward. These results demonstrate that a balanced co-activation of LPO-glutamatergic and LPO-GABAergic inputs to LHb is a critical feature of the normal response to aversive stimuli and suggest that aberrations in this balance can lead to pathological states.

RESULTS

Major Input from the Basal Forebrain to the LHb Is from the LPO Glutamatergic Neurons

The retrograde tracer Fluorogold (FG) was iontophoresed into the LHb to determine the distribution of LHb projection neurons within the basal forebrain (Figures 1A–1C). We found a high concentration of retrogradely labeled FG neurons within the LPO (142.7 ± 12.7 neurons; n = 3 rats; Figure 1C) with fewer FG neurons in the neighboring ventral pallidum (31.3 ± 3.8 neurons), horizontal diagonal band (21.3 ± 6.7 neurons), and medial preoptic area (9.0 ± 4.0 neurons) (Figures S1A and S1B).

We next characterized the phenotype of LPO→LHb neurons by a combination of FG immunodetection and dual *in situ* hybridization for the simultaneous identification of GABA neurons (expressing transcripts encoding glutamic acid decarboxylase (GAD) isoforms 65 and 67, which are enzymes that are responsible for GABA synthesis) (Figure 1D), and glutamate neurons (expressing transcripts encoding the VGluT2, which is a vesicular transporter that accumulates glutamate into synaptic vesicles) (Figure 1E). For dual *in situ* hybridization studies, GADs were initially detected with non-radioactive riboprobes (Figure 1D), and the VGluT2 mRNA with radioactive riboprobes (Figure 1E). We found that most of the LPO→LHb neurons expressed VGluT2 mRNA (FG-VGluT2 neurons: 74.7% ± 3.2%; 322 of a total of 428 FG cells; Figure 1F). A smaller subpopulation of LHb projecting LPO neurons expressed GAD mRNA (FG-GAD neurons: 16.0% ± 3.2%; 68 of 428 FG cells) and very few co-expressed both transcripts (FG-VGluT2^{-}GAD neurons: 3.5% ± 2.8%; 14 of 428 FG^{+} cells) or lacked either transcript (FG-only neurons: 5.9% ± 1.8%; 24 of 428 FG cells). A high proportion of VGluT2 neurons innervating the LHb was also found in ventral pallidum→LHb neurons (VGluT2 neurons: 82.2% ± 8.9%; GAD neurons: 6.1% ± 1.2%) and medial preoptic area→LHb neurons (VGluT2 neurons: 90.0% ± 5.4%; GAD neurons: 7.9% ± 4.0%) but were comparatively much less than the LPO glutamatergic projection to LHb. The proportion of GAD neurons or neurons lacking either transcript that targeted the LHb was greatest in the horizontal diagonal band→LHb neurons (VGluT2 neurons: 41.2% ± 3.5%; GAD neurons: 34.4% ± 8.2%; FG-only neurons: 20.8% ± 2.1%) (Figures S1C and S1D). To exclude the possibility that the infrequent detection of LPO→LHb GAD neurons was due to a suboptimal non-radioactive detection of GAD mRNA, we next used radioactive GAD 65 and 67 riboprobes. By radioactive *in situ* hybridization, we confirmed that only a small subpopulation of LPO→LHb neurons expressed GAD mRNA (25.0% ± 5.2%; 87 of 292 FG cells; Figure 1G). Therefore, our data indicate that most LPO→LHb projection neurons are glutamatergic neurons, which does not support the prevailing notion that the LPO→LHb circuit is predominantly inhibitory (Araki et al., 1984; Garland and Mogenson, 1983; Heimer and Alheid, 1991; Mok and Mogenson, 1972a, 1972b).

LPO→LHb Terminals from Glutamatergic and GABAergic Neurons Have Distinct Topographical Distributions

To determine whether LPO-VGluT2 and LPO-GAD neurons synapse on LHb neurons, we first tagged LPO-VGluT2 neurons by injecting an adeno-associated virus (AAV) encoding Cre-dependent (double fluoxed, inverted orientation [DIO]) channelrhodopsin-2 (ChR2) tethered to mCherry (AAV-DIO-ChR2-mCherry) into the LPO of VGluT2::Cre mice (VGluT2-LPO$^{ChR2\text{-}mCherry}$ mice) and determined, by immunoelectron microscopy, the type of synapses established by these LPO-VGluT2 neurons within the LHb. We found that, within the LHb, axon terminals from LPO-VGluT2 neurons contained VGluT2 protein and established asymmetric synapses (putative excitatory synapses) almost exclusively on dendrites (Figures 2B and 2E; Table S1). In another set of studies, we tagged LPO-GABA neurons by injecting AAV-DIO-ChR2-mCherry into the LPO of VGAT::Cre mice (VGAT-LPO$^{ChR2\text{-}mCherry}$ mice). We found that, within the LHb, axon terminals from LPO-VGAT neurons contained VGAT protein and established symmetric synapses (putative inhibitory synapses) on both dendrites and cell bodies (Figures 2C, 2D, 2F, and 2G; Table S1). These ultrastructural findings indicate that axon terminals from both LPO-glutamate and LPO-GABA neurons synapse on LHb neurons, and each of these terminals contain the necessary molecular machinery for the vesicular accumulation of either glutamate or GABA.

To determine if LPO→LHb neurons release glutamate or GABA onto LHb neurons, we next injected AAV-DIO-ChR2-enhanced yellow fluorescent protein (eYFP) into the LPO of VGluT2::Cre (VGluT2-LPO$^{ChR2\text{-}eYFP}$ mice) or VGAT::Cre mice (VGAT-LPO$^{ChR2\text{-}eYFP}$ mice). LHb photostimulation of LPO-VGluT2 fibers evoked fast, inward, excitatory postsynaptic currents (EPSCs) (Figure 2H), which were abolished by 6-cyano-7-nitroquinoxaline-2,3-dione (CNQX) (an α-amino-3-hydroxy-5-methyl-4-isoxazolepropionic acid [AMPA] receptor

(F) Frequency of different phenotypes of LPO→LHb neurons (mean ± SEM; 10–15 sections from each of three rats). Most LPO→LHb neurons expressed VGluT2 mRNA (FG-VGluT2; 74.7% ± 3.2%), some expressed GADs (FG-GADs; 16.0% ± 3.2%), fewer lacked detectable levels of VGluT2 or GAD mRNA (FG: 5.9% ± 1.8%), and infrequently expressed both transcripts (FG-VGluT2-GADs; 3.5% ± 2.8%).
(G) The frequency of FG-GADs neurons was confirmed with a radioactive probe for GAD 65/67 detection.
Scale bars represent 40 μm in (C) and 10 μm in (D) and (E).

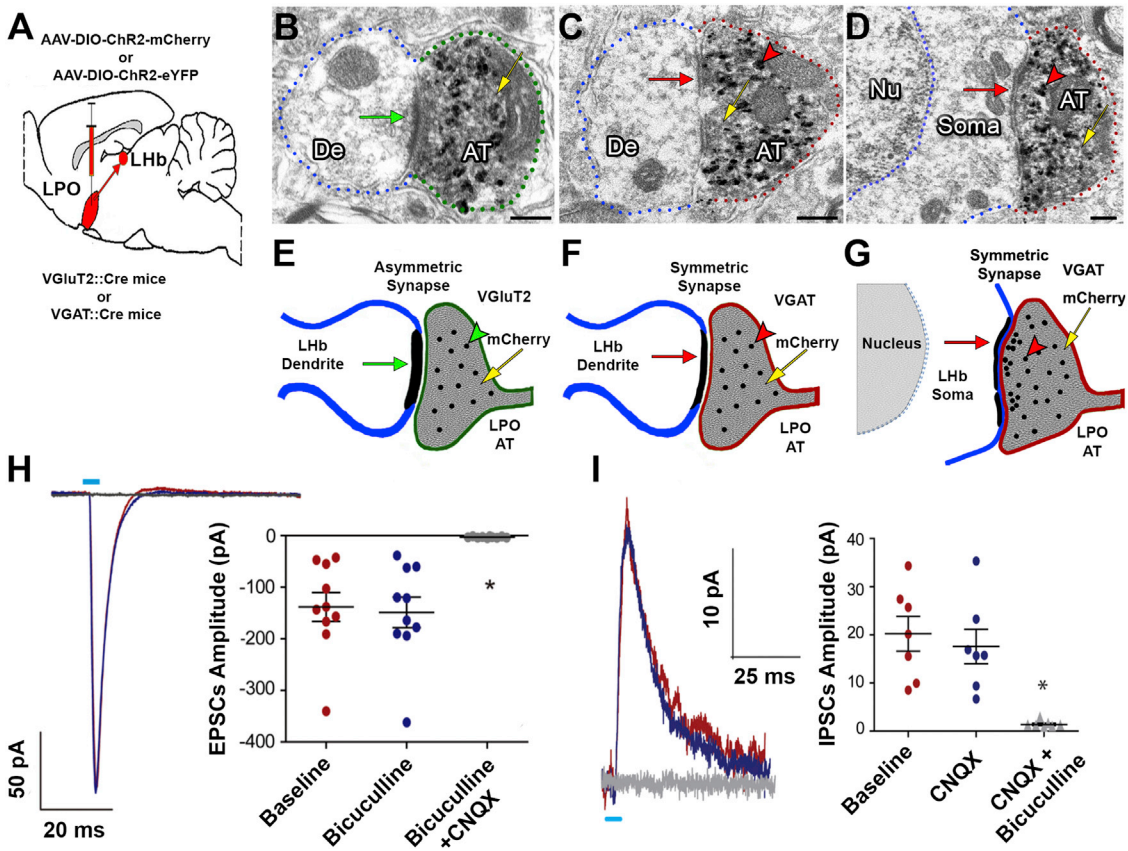

Figure 2. LPO Neurons Establish Functional Glutamate and GABA Synapses on LHb Neurons

(A) Delivery of AAV-DIO-ChR2-mCherry (for electron microscopy) or AAV-DIO-ChR2-eYFP (for *in vitro* electrophysiology) into the LPO of VGluT2::Cre or VGAT::Cre mice.

(B–G) LHb electron micrographs (B–D) and corresponding diagrams (E–G, respectively) showing LPO axon terminals (AT) expressing mCherry (dark, diffuse material; yellow arrow). (B and E) LPO-mCherry terminal in the LHb of a VGluT2-LPO$^{ChR2\text{-}mCherry}$ mouse expressing VGluT2 (labeled using immunogold, which can be seen as dark black puncta; green arrowhead) establishing an asymmetric synapse (green arrow) on a dendrite (De) of an LHb neuron. (C, D, F, and G) LPO mCherry terminal in the LHb of a VGAT-LPO$^{ChR2\text{-}mCherry}$ mouse expressing VGAT (labeled using immunogold, which can be seen as dark black puncta; dots; red arrowheads) establishing a symmetric synapse (red arrow) on a De (C and F) or soma (D and G) of LHb neurons.

(H) EPSCs recorded in voltage-clamp mode in an LHb neuron after LHb photostimulation (blue line) of LPO-VGluT2 fibers were not affected by bicuculline (10 μM) but were abolished by the subsequent addition of CNQX (10 μM) (baseline: −138.18 ± 27.98 pA; bicuculline: −148.83 ± 29.67 pA; bicuculline plus CNQX: −2.84 ± 0.40 pA; [$F_{2,29}$ = 23.56, *p < 0.0001, repeated-measures ANOVA, post hoc Dunnett's test]; n = 10 cells from 6 mice). Error bars correspond to SEMs.

(I) IPSCs recorded in voltage-clamp mode in an LHb neuron after LHb photostimulation (blue line) of LPO-VGAT fibers were not affected by CNQX (10 μM) but were abolished by the subsequent addition of bicuculline (10 μM), (baseline: 20.23 ± 3.60 pA; CNQX: 17.58 ± 3.58 pA; CNQX plus bicuculline: 1.38 ± 0.26 pA [$F_{2,20}$ = 21.56, *p = 0.0001, repeated-measures ANOVA, post hoc Dunnett's test]; n = 7 cells from 5 mice). Error bars correspond to SEMs. Scale bars represent 200 nm in (B)–(D).

antagonist) but were not affected by bicuculline (a $GABA_A$ receptor antagonist) (Figure 2H). LHb single, brief (5-ms) photostimulation of LPO-VGluT2 fibers elicited, in LHb neurons, either single-action potentials or bursts of action potentials (Figure S2B). We also found that tetrodotoxin (TTX) blocked EPSCs that were evoked by photostimulation of LPO-VGluT2 fibers and that EPSCs were restored by the application of 4-aminopyridine (4-AP), thereby confirming that the excitation of LHb neurons by LPO-glutamate release is monosynaptic (Figures S2C and S2D). In contrast, LHb photostimulation of LPO-VGAT fibers evoked fast, outward, inhibitory postsynaptic currents (IPSCs) (Figure 2I), which were completely blocked by bicuculline but were not affected by CNQX (Figure 2I). We showed, via current clamp recordings, that LHb photostimulation of LPO-VGAT fibers resulted in the hyperpolarization of LHb neurons (Figure S3B) and the inhibition of both spontaneous and depolarization-evoked action potentials of LHb neurons (Figures S3C and S3D). Thus, within the LHb, terminals from LPO-VGluT2 neurons establish asymmetric synapses on dendrites, release glutamate, and activate LHb neurons via postsynaptic AMPA receptors. In clear contrast, we found that, within the LHb, terminals from LPO-VGAT neurons synapsed on cell bodies and dendrites, released GABA, and inhibited LHb neurons via postsynaptic $GABA_A$ receptors.

By anterograde tract tracing and immunohistochemistry, we next mapped, within the LHb. the distribution of terminals from

both LPO-VGluT2 and LPO-VGAT terminals. To simultaneously detect LPO-VGluT2 and LPO-VGAT terminals within the LHb, we tagged all LPO neurons, regardless of their phenotype, by injecting, into the LPO of wild-type (WT) C57BL/6J mice, a non-Cre-dependent AAV encoding ChR2 tethered to mCherry (AAV- Ca2+/calmodulin-dependent protein kinase II [CamKII]-ChR2-mCherry) (WT-LPO$^{ChR2\text{-}mCherry}$ mice; Figure 3A). By triple immunofluorescence and confocal microscopy, we then analyzed the distribution of VGluT2-mCherry and VGAT-mCherry axon terminals within the LHb of the WT-LPO$^{ChR2\text{-}mCherry}$ mice (Figures 3B–3D). Although we detected mCherry terminals throughout the LHb, the majority of these terminals (79.1% ± 7.71%; n = 20,068) were concentrated in the medial portion of the LHb, and fewer (20.9% ± 7.36%, n = 4168) were in the lateral portions of the LHb. Within the medial LHb, most of the LPO-mCherry terminals co-expressed VGluT2 (13379 mCherry-VGluT2 terminals; 54.2% ± 2.4%), and fewer co-expressed VGAT (6689 mCherry-VGAT terminals; 24.9% ± 5.3%) (Figures 3C and 3E). However, within the lateral LHb, fewer of the LPO-mCherry terminals co-expressed VGluT2 (1084 mCherry-VGluT2 terminals; 6.1% ± 3.2%), and most expressed VGAT (3084 mCherry-VGAT terminals; 14.8% ± 4.2%; Figures 3D and 3E). Thus, although LPO-glutamatergic and LPO-GABAergic terminals are present throughout the entire LHb, they are concentrated in the medial aspects of the LHb, and their synaptic innervation is topographically distinct. Whereas LPO-GABAergic projections are more broadly distributed within the LHb and may, therefore, exert widespread inhibitory control over the LHb, LPO glutamatergic projections are concentrated within the medial aspects of the LHb (Figures 3E–3G).

LPO-Glutamatergic and LPO-GABAergic Neurons Provide Convergent Neurotransmission onto Single LHb Neurons

Based on the observation that LPO-glutamatergic and LPO-GABAergic terminals are concentrated within the medial aspects of the LHb, we determined, by slice electrophysiology, whether LPO-glutamatergic and LPO-GABAergic neurons synapse on the same LHb neurons. For these studies, we injected, into the LPO of WT C57BL/6J mice, a non-Cre-dependent AAV encoding ChR2 tethered to mCherry (AAV-CaMKIIα-ChR2-mCherry) (WT-LPO$^{ChR2\text{-}eYFP}$ mice; Figure 4A). Whole-cell recordings of LHb neurons were then conducted to determine the proportion of LHb neurons that exhibited both EPSCs and IPSCs after LHb photostimulation of LPO fibers at three holding potentials as follows: −60 mV to record excitatory currents; 0 mV to record inhibitory currents; and −45 mV to record both excitatory and inhibitory currents.

We found that the LHb photostimulation of LPO fibers in ~29% of the recorded LHb neurons produced EPSCs (Figures 4B and 4C), which were blocked by CNQX (an AMPA receptor antagonist), indicating LPO-glutamatergic transmission onto LHb neurons. LHb photostimulation of LPO fibers in ~9% of the recorded LHb neurons produced IPSCs, which were unaffected by CNQX and abolished by bicuculline (a $GABA_A$ receptor antagonist; Figures 4D and 4E), indicating LPO-GABAergic neurotransmission onto LHb neurons. Unexpectedly, a combination of EPSCs and IPSCs was observed in ~62% of the recorded LHb neurons. The initial inward current was completely blocked by CNQX, and the remaining outward current was blocked by the subsequent addition of bicuculline. These results indicate that more than one-half of the LHb neurons that are targeted by the LPO receive convergent LPO-glutamatergic and LPO-GABAergic neurotransmission (Figures 4F and 4G). This unique form of LHb converging glutamatergic and GABAergic neurotransmission is provided by two independent populations of LPO-VGluT2 and LPO-VGAT neurons (Figure 1F), and it is distinct from the LHb glutamatergic-GABAergic co-transmission that has been previously shown to be provided by dually glutamatergic-GABAergic neurons originating from either the VTA (Root et al., 2014b) or EPN (Shabel et al., 2014).

LPO-Glutamate and LPO-GABA Neurons Are Simultaneously Activated during Aversive Conditioning

Although fewer LPO-GABAergic neurons target the LHb than LPO-glutamatergic neurons, our *in vitro* recording experiments demonstrated that LPO-GABAergic transmission converged with LPO-glutamatergic transmission in almost 70% of recorded LHb neurons. Based on this observation, we determined whether both LPO-glutamatergic and LPO-GABAergic neurons play a common role in controlling the excitability of LHb neurons. To accomplish this, we injected an AAV encoding a Cre-dependent GCAMP6s into the LPO of VGluT2::Cre (VGluT2-LPO^{GCAMP6s} mice) or VGAT::Cre mice (VGAT-LPO^{GCAMP6s} mice) and implanted an optic fiber over the LHb to record Ca^{2+} transients specifically from LPO-VGluT2 or LPO-VGAT axons in the LHb during classical conditioning tasks for a sucrose reward or footshock. In these tasks, a 5-s conditioned stimulus (CS)+ tone or CS+ white noise signaled the delivery of either 25 μL of 8% sucrose or a 0.85-mA, 0.1-s footshock (Figures 5A, 5B and S4A).

We observed that both LPO-VGluT2 and LPO-VGAT axons in the LHb significantly increased Ca^{2+} activity (%$\Delta F/F$) after presentation of an aversive footshock as well as by a cue predicting its delivery (Figures 5C–5F). Further, the activation of LPO-VGluT2 and LPO-VGAT was balanced as there was no difference in the amplitude of Ca^{2+} responses that were recorded between LHb LPO-VGluT2 and LPO-VGAT fibers. In contrast to the observed increase in the amplitude of Ca^{2+} activity during aversive conditioning, we found that neither the consumption of sucrose nor a cue predicting its delivery elicited a measurable activation of LPO-VGluT2 or LPO-VGAT fibers in the LHb (Figure S4).

Independent Photostimulation of LPO-VGluT2 or LPO-VGAT Axons in LHb Differentially Drives Motivated Behavior

Recorded Ca^{2+} responses indicated that LPO-VGluT2 and LPO-VGAT axons in the LHb were simultaneously activated by an aversive footshock and a cue predicting its delivery. We next determined whether perturbing this balance by independently driving only LPO-glutamate or driving only LPO-GABA was sufficient to alter motivated behaviors.

To determine the behavioral consequences of independently activating LPO-glutamatergic inputs to the LHb, we injected, into the LPO of VGluT2::Cre mice, either AAV-DIO-ChR2-eYFP

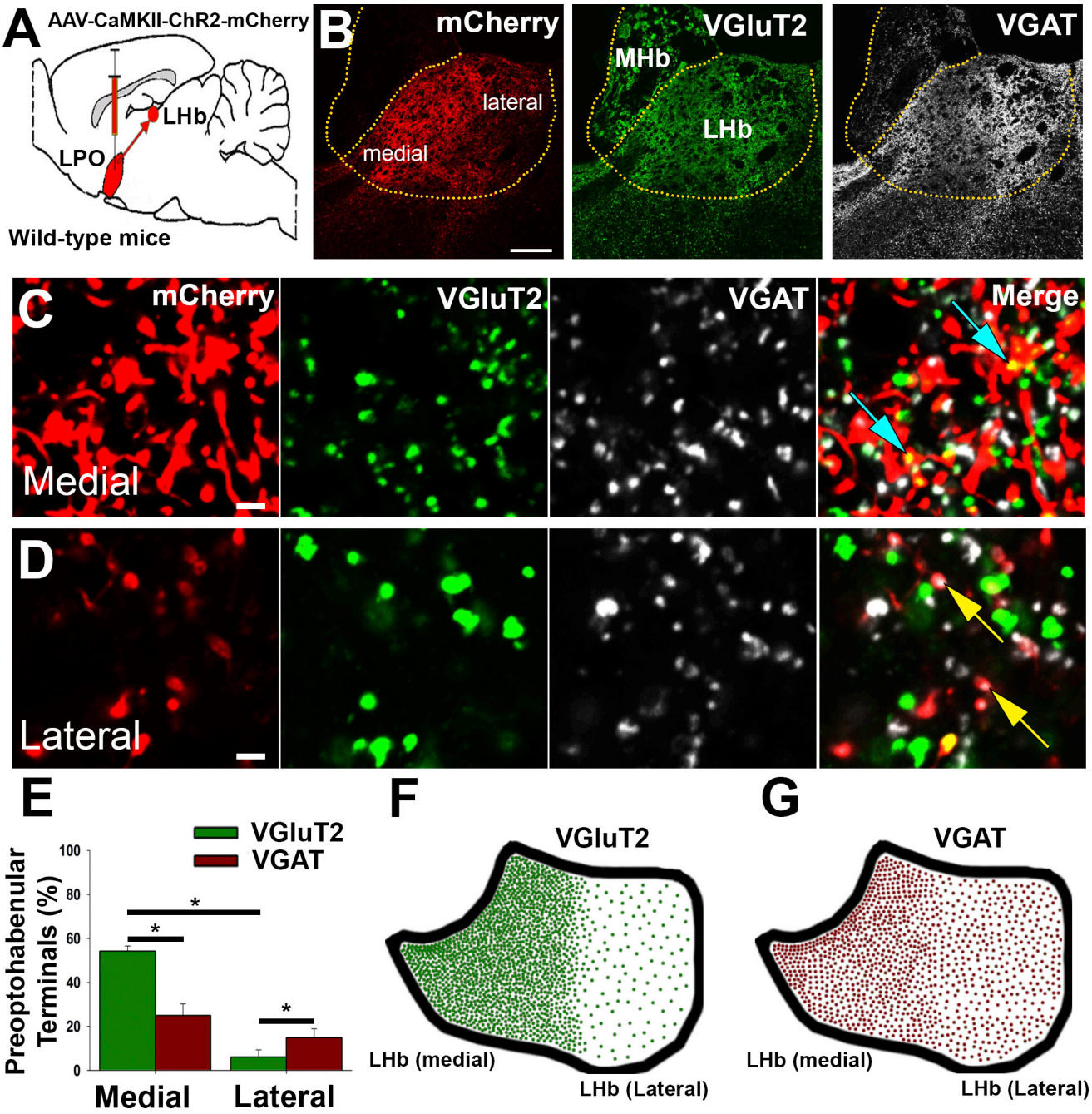

Figure 3. Axon Terminals from LPO-Glutamate and LPO-GABA Neurons Innervating the LHb Have Distinct Topographical Distributions within the LHb

(A) Delivery of AAV-CaMKII-ChR2-mCherry into the LPO of wild-type mice (WT-LPO$^{ChR2\text{-}mCherry}$).

(B) LHb at low magnification showing LPO-mCherry fibers in the LHb and axon terminals with either VGluT2 or VGAT labeling.

(C and D) High magnification of the medial (C) and lateral (D) aspects of the LHb showing LPO terminals containing VgluT2 (blue arrows) or VGAT (yellow arrows).

(E) LPO-mCherry fibers were more prevalent in the medial than in the lateral aspects of the LHb and more frequently contained VgluT2 than VGAT. Within the lateral aspects of the LHb, the LPO-mCherry-VGAT were more abundant than were LPO-mCherry-VGluT2 (n = 24,236 terminals; n = 3 mice with three replications each [$F_{1,8}$ = 49.02, p = 0.0001, two-way repeated-measures ANOVA, Sidak adjusted post hoc, *p < 0.05]). Data are shown as mean ± SEM.

(F and G) Diagrams showing a high concentration of LPO-mCherry-VGluT2 axon terminals in the medial aspect of the LHb (F) and a broad distribution of LPO-mCherry-VGAT axon terminals across the LHb (G).

Scale bars represent 100 μm in (B) and 2 μm in (C) and (D).

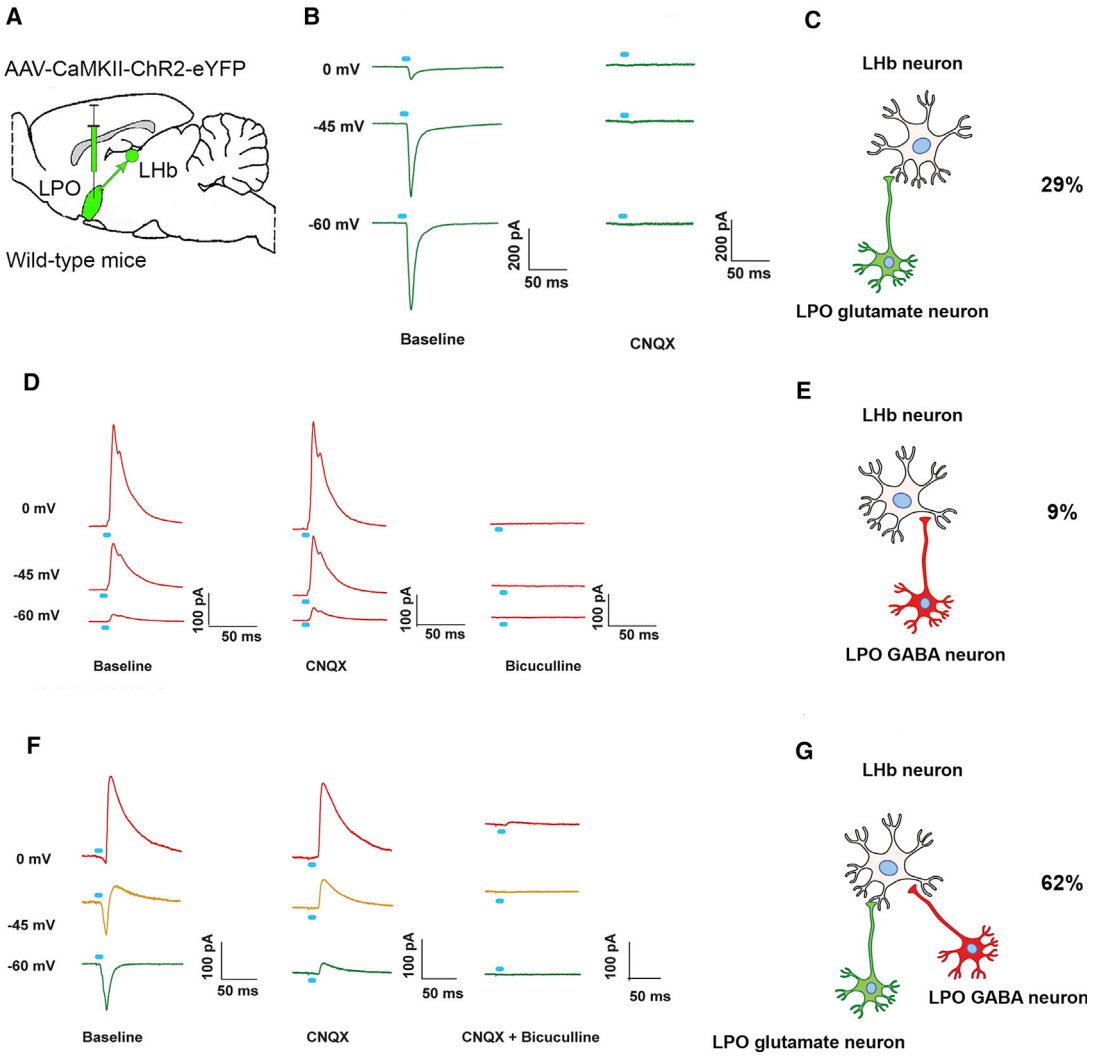

Figure 4. Converging LPO-Glutamatergic and LPO-GABAergic Inputs onto Single LHb Neurons

(A) Delivery of AAV-CaMKII-ChR2-eYFP into the LPO of wild-type mice (WT-LPO$^{ChR2\text{-}eYFP}$).

(B and C) LPO-glutamatergic input on an LHb neuron. EPSCs recorded in voltage-clamp mode in an LHb neuron at three holding potentials after LHb photostimulation (blue line) of LPO-fibers were all blocked by CNQX (10 μM) (B) indicating LPO-glutamatergic neurotransmission on LHb neurons (~29%; 6 of 21 recorded LHb neurons) (C).

(D and E) LPO-GABAergic input on an LHb neuron. IPSCs recorded in voltage-clamp mode at three holding potentials in an LHb neuron after LHb photostimulation (blue line) of LPO-fibers were not affected by CNQX (10 μM) but were all blocked by the subsequent addition of bicuculline (10 μM) (D) indicating LPO-GABAergic neurotransmission on LHb neurons (~9%; 2 of 21 recorded LHb neurons) (E).

(F and G) Convergent neurotransmission of LPO-glutamate and LPO-GABA inputs on a single LHb neuron. Both EPSCs and IPSCs were recorded in voltage-clamp mode on a single LHb neuron after LHb photostimulation. EPSCs were blocked by CNQX (10 μM), and the remaining IPSCs were blocked by the subsequent addition of bicuculline (10 μM) (F) indicating that LPO-glutamate and LPO-GABA neurons provide convergent neurotransmission onto single LHb neurons (~62%; 13 of 21 recorded LHb neurons) (G).

(B, D, and F) LHb neurons were recorded under voltage clamp at three holding potentials: 0 mV to record inhibitory currents; −60 mV to record excitatory currents, and −45 mV to simultaneously record both inhibitory and excitatory currents.

(VGluT2-LPO$^{ChR2\text{-}eYFP}$ mice) or AAV-DIO-eYFP (VGluT2-LPO^{eYFP} mice), and an optic fiber was implanted over the LHb to optogenetically activate LPO-VGluT2 axons (Figures 6A and S5A). VGluT2-LPO$^{ChR2\text{-}eYFP}$ and VGluT2-LPO^{eYFP} mice were tested in a three-chamber apparatus with two pairing chambers and one connecting chamber. In this real-time place-conditioning procedure, continuous trains of 20 Hz photostimulation were delivered when mice entered a photostimulation-paired chamber and were terminated when mice exited the chamber (Figure 6B). VGluT2-LPO^{eYFP} mice spent a similar time in both the photostimulation-paired and unpaired chambers throughout the experiment. In contrast, VGluT2-LPO$^{ChR2\text{-}eYFP}$ mice avoided the photostimulation-paired chamber, spending significantly more time in the photostimulation-unpaired chamber (pairings

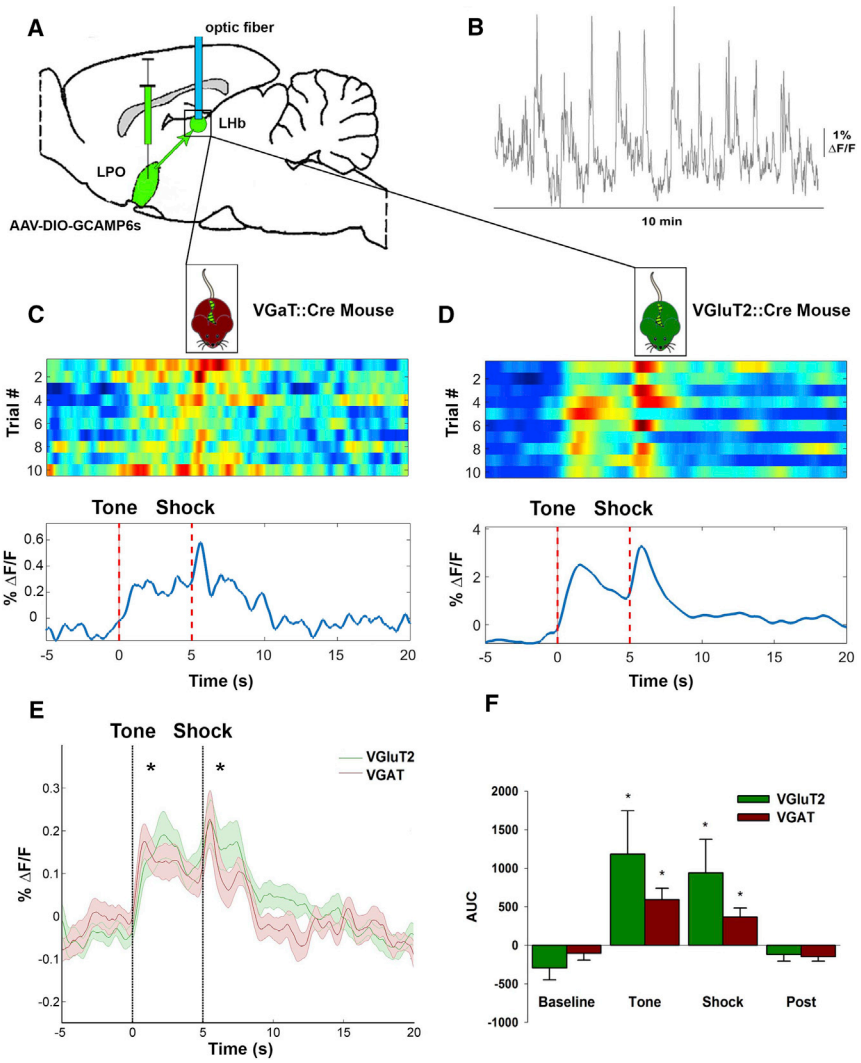

Figure 5. Simultaneous Activation of LPO-VGluT2 and LPO-VGAT Fibers in the LHb by an Aversive Stimulus and Its Predictive Cue

(A) Delivery of AAV-DIO-GCAMP6s into the LPO in VGAT-LPO^{GCaMP6s} mice or VGluT2-LPO^{GCaMP6s} mice and optic fiber placement over the LHb for recording Ca^{2+} activity in LPO-VGluT2 fibers and LPO-VGAT fibers.

(B) Ca^{2+}-imaging traces during an entire aversive conditioning task.

(C and D) Heatmaps of Ca^{2+} activity over successive aversive conditioning trials (top) and peri-event histograms showing the average trace during aversive conditioning (bottom) in a VGAT-LPO^{GCaMP6s} mouse (C) and VGluT2-LPO^{GCaMP6s} mouse (D).

(E) Average ± SEM Ca^{2+} activity for VGluT2-LPO^{GCaMP6s} mice or VGAT-LPO^{GCaMP6s} mice in a 25-s window encompassing the tone and foot-shock periods.

(F) Area under the curve ($\Delta F/F$) for Ca^{2+} activity in LPO-VGluT2 terminals or LPO-VGAT terminals during baseline (VGluT2-LPO^{GCaMP6s} mice: −293.52 ± 155.47; VGAT-LPO^{GCaMP6s} mice: −103.12 ± 91.13), tone (VGluT2-LPO^{GCaMP6s} mice: 1183.86 ± 562.63; VGAT-LPO^{GCaMP6s} mice: 590.88 ± 149.85), shock (VGluT2-LPO^{GCaMP6s} mice: 940.03 ± 434.93; VGAT-LPO^{GCaMP6s} mice: 365.13 ± 116.72), and post-shock epochs (VGluT2-LPO^{GCaMP6s} mice: −121.05 ± 85.55; VGAT-LPO^{GCaMP6s} mice: −147.96 ± 58.50) (n = 13 VGluT2-LPO^{GCaMP6} mice, and n = 14 VGAT-LPO^{GCaMP6} mice [mixed ANOVA, main effect of epoch: $F_{3,75}$ = 24.61, p < 0.0001, general linear model [GLM], Sidak post hoc test,*p < 0.001 versus baseline; epoch × group and group effects: not significant).

1–4: all p < 0.05). When subsequently tested in the absence of laser stimulation, VGluT2-LPO$^{ChR2\text{-}eYFP}$ mice exhibited a significant place aversion toward the laser-paired chamber (p < 0.05). Reversing the photostimulation contingencies by pairing the stimulation of LPO-VGluT2 fibers with the opposite chamber resulted in a concomitant reversal of photostimulation-avoidance behavior (reversals 1–4: all p < 0.05) and in a significant place aversion to this chamber during a stimulation-free test session (p < 0.05) (Figure 6C). Thus, the independent activation of LPO-glutamatergic inputs to the LHb is aversive.

To determine the behavioral consequences of independently activating LPO-GABAergic inputs to the LHb, we injected, into the LPO of VGAT::Cre mice, either AAV-DIO-ChR2-eYFP (VGAT-LPO$^{ChR2\text{-}eYFP}$ mice) (Figure 6A) or AAV-DIO-eYFP (VGAT-LPO^{eYFP} mice), and an optic fiber was placed over the LHb for the photostimulation of LPO-VGAT fibers (Figure S5A). VGAT-LPO$^{ChR2\text{-}eYFP}$ and VGAT-LPO^{eYFP} mice were tested in the real-time place-conditioning task. VGAT-LPO^{eYFP} mice spent similar time in both the photostimulation-paired and unpaired chambers throughout the experiment. However, VGAT-LPO$^{ChR2\text{-}eYFP}$ mice spent significantly more time in the photostimulation-paired chamber in pairing sessions 1, 2, and 4 (all p < 0.05; pairing 3: p = 0.08). Reversing the photostimulation pairing to the opposite chamber caused mice to switch their preference to the side that was newly paired with photostimulation (reversals 1–4: all p < 0.05) (Figure 6D). Unlike VGluT2-LPO$^{ChR2\text{-}eYFP}$ mice, VGAT-LPO$^{ChR2\text{-}eYFP}$ mice did not show a conditioned preference or aversion for the previously stimulation-paired chamber during stimulation-free test sessions. Thus, the independent activation of LPO-GABAergic inputs to the LHb promotes a place preference but not a conditioned reward.

VGluT2-LPO$^{ChR2\text{-}eYFP}$ and VGluT2-LPO^{eYFP} mice were then tested in a shuttle-avoidance task to assess if mice would shuttle to escape LHb photostimulation of LPO-VGluT2 fibers. VGluT2-LPO$^{ChR2\text{-}eYFP}$ mice escaped LHb photostimulation of LPO-VGluT2 fibers significantly more often than did VGluT2-LPO^{eYFP} control mice at each of five counterbalanced test frequencies (5, 10, 20, 40, and 80 Hz; main effect of group: p < 0.001) (Figure S5B). To confirm that LHb photostimulation of LPO-VGAT fibers supports reward, VGAT-LPO$^{ChR2\text{-}eYFP}$ and VGAT-LPO^{eYFP}

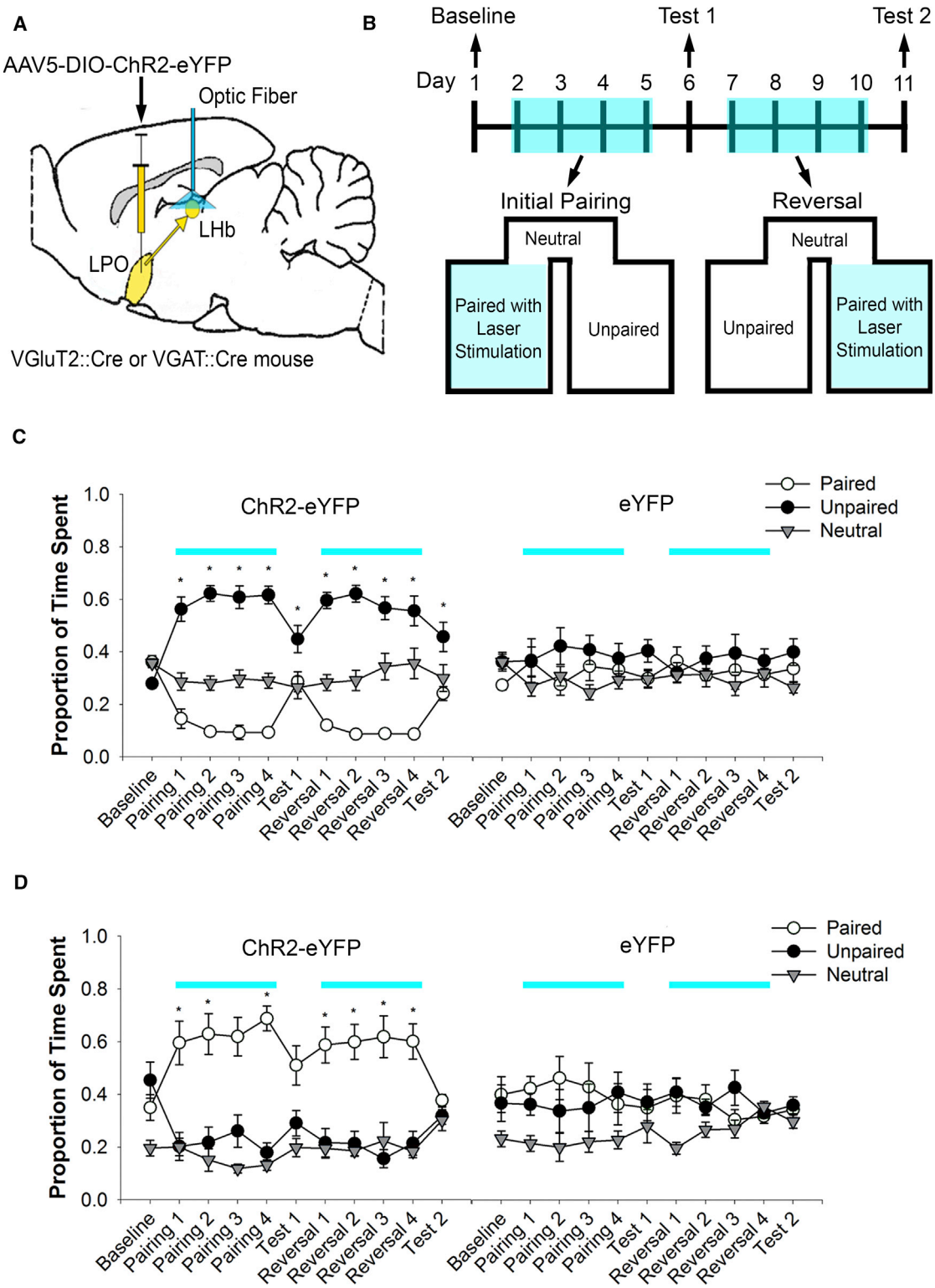

Figure 6. LHb Photostimulation of LPO-Glutamate Is Aversive, whereas LHb Photostimulation of LPO-GABA Fibers Is Rewarding

(A) Diagram of virus injection in LPO and photostimulation of LPO-VGluT2 or LPO-VGAT fibers in the LHb.

(B) Timeline for the place conditioning procedure.

(legend continued on next page)

mice were tested in a shuttle reward task. Shuttle responses to earn LHb photostimulation of LPO-VGAT fibers were significantly greater in VGAT-LPO$^{ChR2\text{-}eYFP}$ mice than in VGAT-LPO^{eYFP} mice at each of five counterbalanced test frequencies (5, 10, 20, 40, and 80 Hz; main effect of group: $p < 0.05$) (Figure S5C). Thus, mice will work to avoid photostimulation of LPO-VGluT2 inputs to the LHb and will work to earn photostimulation of LPO-VGAT inputs to the LHb. We therefore conclude that the independent activation of LPO-glutamatergic inputs to the LHb is aversive while the independent activation of LPO-GABAergic inputs to the LHb is rewarding.

To further evaluate the effects of independent activation of LPO-glutamate and LPO-GABA on LHb neuronal activity, we quantified c-Fos expression (a marker of neuronal activation) in the LHb after LHb photostimulation of either LPO-VGluT2 or LPO-VGAT fibers. To accomplish this, VGluT2-LPO$^{ChR2\text{-}eYFP}$, VGluT2-LPO^{eYFP}, VGAT-LPO$^{ChR2\text{-}eYFP}$, and VGAT-LPO ^{eYFP} mice were placed in an open field and given intermittent LHb photostimulation (5-s trains delivered every 15 s) for a period of 15 min. When compared to eYFP control mice, VGluT2-LPO$^{ChR2\text{-}eYFP}$, but not VGAT-LPO$^{ChR2\text{-}eYFP}$ mice, exhibited increases in the number of c-Fos-positive cells within the LHb ($p < 0.001$). Further, the number of c-Fos-positive cells in VGluT2-LPO$^{ChR2\text{-}eYFP}$ mice was higher than in VGAT-LPO$^{ChR2\text{-}eYFP}$ mice ($p < 0.05$). The number of neurons expressing c-Fos in VGluT2-LPO^{eYFP} and VGAT-LPO^{eYFP} mice did not increase (Figures S5D–S5H). Thus, we conclude that LHb photostimulation of LPO-VGluT2 fibers leads to the site-specific activation of LHb neurons.

DISCUSSION

The LHb has been implicated in addiction and depression, among other mental disorders (Jhou et al., 2013; Li et al., 2011; Meye et al., 2016; Shabel et al., 2014; Yang et al., 2008), which may result from alterations of LHb neuronal signaling at the molecular, cellular, or neurocircuitry levels. Recent studies have demonstrated that cell-specific inputs to LHb from the VTA, EPN, and LH participate in different aspects of behavior (Root et al., 2014a; Shabel et al., 2014; Stamatakis et al., 2016; Stephenson-Jones et al., 2016). Regarding other inputs to the LHb, it has been established that the LPO provides one of the largest inputs to the LHb (Yetnikoff et al., 2015), but the composition of this input and its specific role in regulating LHb function have remained unclear (Proulx et al., 2014). Here, we demonstrate that most LPO→LHb neurons are glutamatergic and fewer are GABAergic, which challenges the predicted view of a major LPO→LHb GABAergic input. We identified that a subset of LPO projections to LHb are GABAergic. Further, we discovered that the LPO→LHb inputs control the activity of LHb neurons through an unexpected mechanism of converging LPO-glutamatergic and LPO-GABAergic neurotransmission onto single LHb neurons. In addition, we found that the concurrent activation of LPO-glutamatergic and LPO-GABAergic inputs to the LHb occurs in response to an aversive footshock and its learned predictor. Moreover, we discovered that perturbing the balanced release of glutamate and GABA through the independent optogenetic activation of either LPO-glutamate or LPO-GABA shifted motivated behavior between reward and aversion (Figure 7).

Role for the LPO→LHb Circuit in the Processing of Noxious Stimuli

Recent optogenetic behavioral studies have demonstrated that LHb activation of glutamatergic inputs from the VTA (Root et al., 2014a), LH (Stamatakis et al., 2016), or EPN (Shabel et al., 2012) results in behavioral avoidance and is aversive. In contrast, LHb activation of projections from VTA GABA-tyrosine-hydroxylase neurons (Stamatakis et al., 2013) results in behavioral approach and is rewarding.

While the overall result of LHb activation or inhibition appears to be consistent across LHb inputs, we are just beginning to understand the specific types of information that are carried by each LHb input. For instance, LH→LHb glutamatergic neurotransmission may encode information related to hunger and satiety as the inhibition of these neurons increases caloric consumption (Stamatakis et al., 2016). In contrast, EPN→LHb neurons were recently shown to encode information about the outcomes of behavioral actions as these cells show a graded level of inhibition or excitation depending on how good or bad an outcome is relative to what was expected (Stephenson-Jones et al., 2016).

Here, we demonstrate that LPO-glutamate neurons and LPO-GABA projections to LHb participate in encoding the neural response to noxious stimuli and their predictive cues. However, in clear contrast to the adjacent LH→LHb neurons (Stamatakis et al., 2016), we did not find evidence that LPO→LHb projections are modulated by appetitive stimuli or ingestive behavior. On the basis of these findings and evidence implicating the LPO in the corticosterone response to acute restraint stress (Duarte et al., 2017) or acute pain (Burstein et al., 1987), we propose that the LPO provides the LHb with information that is related to the peripheral and neuroendocrine responses to noxious stimuli.

Critical Balance between LHb Glutamatergic and GABAergic Neurotransmission

A previous quantitative analysis of random LHb axon terminals containing VGluT2 or VGAT demonstrated that ≈53% of single axon terminals co-express VGluT2 and VGAT (Root et al., 2014b). These dual glutamatergic-GABAergic axon terminals

(C) VGluT2-LPO$^{ChR2\text{-}eYFP}$ mice (n = 9) spent less time in the chamber paired with photostimulation on conditioning days (blue line) and exhibited place aversion during stimulation-free test sessions. VGluT2-LPO^{eYFP} mice (n = 7) spent equal time in the photostimulation paired and unpaired chambers during conditioning (blue line) and test sessions ($F_{20,280} = 3.78$, $p < 0.0001$, mixed ANOVA, Sidak adjusted post hoc, *$p < 0.05$ for paired versus unpaired chambers).
(D) VGAT-LPO$^{ChR2\text{-}eYFP}$ mice (n = 7) spent more time in the photostimulation paired chamber during conditioning (blue line) sessions. Stimulation in VGAT-LPO$^{ChR2\text{-}eYFP}$ mice did not produce a conditioned place preference for the photostimulation-paired chamber on test sessions, although there was a trend for animals to spend more time in the photostimulation paired chamber. VGAT-LPO^{eYFP} mice (n = 7) did not show a preference for either the paired or unpaired chamber during conditioning sessions (blue line) or test sessions ($F_{20,260} = 1.76$, $p = 0.26$, mixed ANOVA, Sidak-adjusted post hoc, *$p < 0.05$ for paired versus unpaired chambers). Data are shown as mean ± SEM.

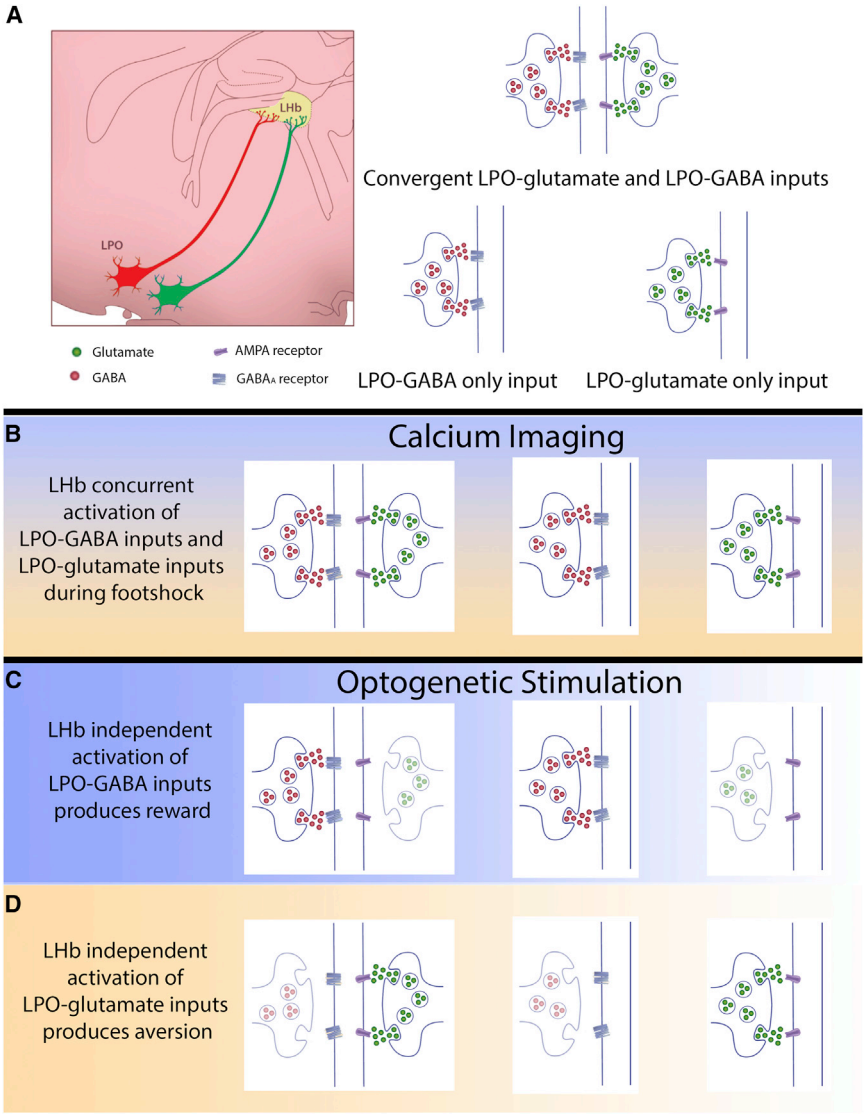

Figure 7. Functional Neuroanatomy of the LPO→LHb Circuit

(A) Electrophysiological and anatomical evidence indicate that LPO-glutamate and LPO-GABA neurons both synapse on single LHb neurons to provide convergent neurotransmission of glutamate and GABA or independently synapse on LHb neurons to release only glutamate or only GABA.

(B) Recording LPO-VGluT2 or LPO-VGAT terminals by fiber photometry Ca^{2+} imaging demonstrated that noxious footshock induces the simultaneous and balanced activation of LPO-glutamatergic and LPO-GABAergic inputs to the LHb.

(C and D) Independent optogenetic activation of LPO→LHb GABA produces reward (C) while independent optogenetic activation of LPO→LHb glutamate produces aversions (D). These results suggest that the balance of LPO-glutamate and LPO-GABA is critical for an organisms' normal response to aversive stimuli and that shifts in this balance may produce a psychopathological state.

have been shown to be derived from co-releasing glutamatergic-GABAergic neurons that are located in both the EPN (Shabel et al., 2014) and VTA (Root et al., 2014b). In addition to the major subpopulation of LHb dual-glutamatergic-GABAergic terminals, the LHb has subpopulations of terminals that contain only VGluT2 (≈33% of the terminals) or only VGAT (≈13% of the terminals). Here, we demonstrated that a fraction of the LHb axon terminals providing either glutamatergic-only or GABAergic-only neurotransmission are derived from independent populations of LPO-glutamate and LPO-GABA neurons. Moreover, we discovered that, contrary to the prevailing idea that LPO→LHb inputs are mostly GABAergic, most LPO→LHb neurons are glutamatergic and fewer are GABAergic neurons. Nonetheless, in characterizing this circuit, we discovered an unexpected mechanism of convergent neurotransmission by which independent populations of LPO-glutamatergic and LPO-GABAergic neurons synapsed and released either glutamate or GABA or both onto the same LHb neuron. This mechanism allows for different inputs to LPO-glutamate or LPO-GABA neurons to differentially influence the LHB glutamatergic or GABAergic tone, which represents a mechanism in which long-range inputs from the same brain area but from different neurons can exert bivalent control over LHb neurons. This intriguing mechanism contrasts with the bivalent control that is provided by the co-release of glutamate and GABA from single axon terminals from either the VTA or EPN.

The LHb has been proposed to play a role in the integration of information about behavioral outcomes, bodily states, and environmental stimuli and in the evaluation of this information to guide motivated behavior (Baker et al., 2016; Kawai et al., 2015; Matsumoto and Hikosaka, 2007; Stopper and Floresco, 2014). In addition, several studies have demonstrated that changes in the balance of glutamatergic and GABAergic integrations by the LHb are associated with mental disorders (Maroteaux and Mameli, 2012; Meye et al., 2016; Shabel et al., 2014). Here, we demonstrated, by *in vivo* calcium recordings, the simultaneous and balanced activation of LPO-glutamatergic and LPO-GABAergic neurons during the processing of noxious stimuli. Further, we demonstrated, by optogenetic stimulation, that independently activating of LPO-glutamate or LPO-GABA neurons is sufficient to shift an animal's state between reward and aversion, suggesting that the balance of LPO-glutamate and LPO-GABA is critical for an organism's normal response to noxious stimuli. Accordingly, shifts in this balance may lead to aberrant responses to environmental stimuli and produce a psychopathological state, underlying the need of having a better understanding of the LPO→LHb circuitry to

determine its possible role in addiction, depression, schizophrenia, or other LHb-related psychopathologies.

EXPERIMENTAL PROCEDURES

Animals

Male Sprague Dawley rats (12–18 weeks old; 300–500 g; Charles River Laboratories) were used for Fluorogold retrograde tracing. Male WT VGluT2::Cre mice (6–12 weeks old; 20–35 g; Borgius et al., 2010) or VGAT-internal ribosomal entry site (IRES)::Cre mice (6–12 weeks old; 20–35 g; Slc32a1tm2(Cre)Lowl/J in a C57BL/6J background from The Jackson Laboratories; RRID IMSR_JAX:016962) were used for confocal microscopy, electron microscopy, and electrophysiological and behavioral experiments. All animal procedures were performed in accordance with NIH guidelines and approved by the National Institute on Drug Abuse (NIDA) animal care and use committee.

Surgery

Stereotaxic surgeries for virus injections or fiber optic implants were performed under isofluorane as described previously (Root et al., 2014a). Viruses that were used in microscopy, electrophysiology, or behavioral experiments were targeted to the LPO (+0.5 AP, −2.0 ML, −5.4 DV; 10°), and optic fibers were implanted dorsal to the LHb (−1.6 AP, −1.0 ML, −2.7 DV; 9°). For details, see Supplemental Experimental Procedures.

In Situ Hybridization

Hybridization was performed either by single *in situ* hybridization for radioactive detection of *GAD* mRNA (transcripts encoding the two isoforms of GAD [i.e., *GAD65* or *GAD67*] or double *in situ* hybridization for radioactive detection of *VGluT2* mRNA or nonradioactive detection of *GAD* mRNA as previously detailed (Root et al., 2014b; Yamaguchi et al., 2007, 2011). For details, see Supplemental Experimental Procedures.

Whole-Cell Electrophysiological Recordings

LHb neurons from 200-μM coronal slices from VGluT2::Cre or VGAT::Cre mice injected with AAV5-eukarytoci translation elongation factor 1 alpha (Ef1α)-ChR2-eYFP virus or WT mice injected with AAV5-CAMKII-ChR2-eYFP were recorded in modified artificial cerebrospinal fluid (ACSF) containing 125 mM NaCl, 2.5 mM KCl, 1.25 mM NaH_2PO_4, 1 mM $MgCl_2$, 2.4 mM $CaCl_2$, 26 mM $NaHCO_3$, and 11 mM glucose (pH 7.4). Neurons were visualized on an upright microscope using infrared differential-interference-contrast video microscopy and patched with electrodes (4–6 MΩ) backfilled with either a potassium gluconate internal solution containing 140 mM potassium gluconate, 2 mM NaCl, 1.5 mM $MgCl_2$, 10 mM HEPES, 4 mM Mg-ATP, 0.3 mM Na_2-guanosine-triphosphate, 10 mM Na-phosphocreatine, 0.1 mM EGTA, and 0.2% biocytin (pH 7.2; 280–290 mOsm). When testing for the convergent neurotransmission of glutamate and GABA, a cesium methansulfonate internal solution containing 124 mM $CsMeSO_4$, 11 mM KCl, 0.1 mM EGTA, 10 mM HEPES, 10 mM Na_2 phosphocreatine, 4 MgATP, 0.3 Na_2GTP, and 0.5% biocytin (pH 7.2; 280 mOsm) was used. A 200-μm core optical fiber, which was coupled to a diode-pumped solid state laser, was positioned just above the slice and aimed at the recorded cell. Optically evoked EPSCs or IPSCs were obtained every 10 s with pulses of 473-nm wavelength light (8 mW, 5 ms). The peak amplitude of EPSCs or IPSCs was measured with the average of 30 consecutive traces. EPSCs from VGluT2:Cre mice were recorded at −60 mV while IPSCs from VGAT::Cre mice were recorded at −45 mV. When testing for convergent neurotransmission of glutamate and GABA, LHb neurons were held at three different voltages (−60, −45, and 0 mV). Current clamp recordings were made by switching from voltage-clamp mode to current-clamp mode after the pharmacological isolation of EPSCs or IPSCs.

Confocal and Electron Microscopy

Vibratome sections of the LHb were obtained from three VGluT2-LPO$^{ChR2\text{-}mCherry}$ or three VGAT-LPO$^{ChR2\text{-}mCherry}$ mice. Free-floating sections were double or triple immunolabeled with antibodies for the detection of mCherry and VGluT2, VGAT, or both VGluT2 and VGAT. For electron microscopy, serial ultrathin sections of the LHb were then taken, and synaptic contacts were classified according to their morphology and then immunolabeled and photographed at a magnification of 6,800–13,000×. For confocal microscopy, z-axis stacks of fluorescent images and serial electron microscopic images were analyzed as previously detailed (Zhang et al., 2015). For details, see Supplemental Experimental Procedures.

Real-Time Place Conditioning

Using the three-chamber place conditioning apparatus, VGluT2-LPO$^{ChR2\text{-}eYFP}$, VGluT2-LPO^{eYFP}, VGAT-LPO$^{ChR2\text{-}eYFP}$, and VGAT-LPO^{eYFP} mice were subsequently tested to determine if photostimulation would produce place conditioning or place aversion as described previously (Root et al., 2014a). Briefly, mice were given light stimulation through the optic fiber (473 nm, ~7 mW, 10-ms duration, 20 Hz) in the LHb whenever they entered the photostimulation-paired chamber. Mice were then tested for a place preference in the absence of photostimulation. After the first stage of conditioning, photostimulation was shifted to the opposite conditioning chamber for four conditioning chambers (reversal sessions 1–4). Upon completion of reversal training, mice were again tested in the absence of photostimulation. All experimental procedures were controlled by video-tracking software (AnyMazel Stoelting). For details, see Supplemental Experimental Procedures.

Fiber Photometry

Ca^{2+} signals from VGluT2-LPO^{GCaMP6} and VGAT-LPO^{GCaMP6} mice, with 400-μm optic fibers implanted over LPO fibers in the LHb, were recorded during classical conditioning tasks for a sucrose reward or footshock. In these tasks, a 5-s CS+ tone or CS+ white noise signaled the delivery of either 25 μL of 8% sucrose or a 0.85-mA, 0.1-s footshock. For all recordings, GCaMP6s was excited at two wavelengths (490-nm calcium-dependent signal and 405-nm isosbestic control (Lerner et al., 2015). An analysis of the resulting signal was then performed using custom-written MATLAB scripts. Changes in fluorescence across the experimental session ($\Delta F/F$) were calculated by smoothing signals from the isosbestic control channel (Lerner et al., 2015), scaling the isosbestic control signal by regressing it on the smoothed GCaMP signal, and generating a predicted 405-nm signal using the linear model that was generated during the regression. Calcium-independent signals on the predicted 405-nm channel were then subtracted from the raw GCAMP signal to remove movement, photo-bleaching, and fiber-bending artifacts. Signals from the GCaMP channel were then divided by the control signal to generate the $\Delta F/F$. Peri-event histograms were then created by averaging changes in fluorescence ($\Delta F/F$) across repeated trials during windows encompassing behavioral events of interest.

Statistics

One- and two-way ANOVAs were used to compare between-group effects, repeated-measures ANOVAs were used to compare within-group effects across time, and a mixed ANOVA was used for analyses with both within- and between-subjects factors. For additional details, see Supplemental Experimental Procedures.

SUPPLEMENTAL INFORMATION

Supplemental Information includes Supplemental Experimental Procedures, five figures, and one table can be found with this article online at https://doi.org/10.1016/j.celrep.2017.10.066.

AUTHORS CONTRIBUTIONS

D.J.B. and M.M. wrote the manuscript and participated in the conception and design of all experiments. J.M.B, S.Z., D.H.R, H.-L.W., B.L., and E.S.C. participated in the writing of the manuscript; D.J.B., H.-L.W., B.L., and D.H.R. conducted and quantified *in situ* hybridization studies. J.M.B. conducted *in vitro* electrophysiological experiments. S.Z. conducted confocal and electron microscopy experiments. E.S.C. and D.J.B. participated in the design and analysis of photometry experiments. D.J.B. conducted all photometry and optogenetics experiments.

ACKNOWLEDGMENTS

We thank Drs. Carlos Mejias-Aponte, Jia Qi, and Roy Wise for their feedback and Rong Ye for her help in processing brain tissue. We also thank the visual media department at the NIDA Intramural Research Program (IRP) for assistance in the preparation of figures. The IRP of the NIDA, US NIH (IRP/NIDA/NIH), supported this work. D.J.B. was supported by K99 DA043572. E.S.C. was supported by NIDA K99 DA042111 and the Brain and Behavior Research Foundation.

Received: March 20, 2017
Revised: September 6, 2017
Accepted: October 18, 2017
Published: November 14, 2017

REFERENCES

Aizawa, H., Cui, W., Tanaka, K., and Okamoto, H. (2013). Hyperactivation of the habenula as a link between depression and sleep disturbance. Front. Hum. Neurosci. *7*, 826.

Araki, M., McGeer, P.L., and McGeer, E.G. (1984). Retrograde HRP tracing combined with a pharmacohistochemical method for GABA transaminase for the identification of presumptive GABAergic projections to the habenula. Brain Res. *304*, 271–277.

Baker, P.M., Jhou, T., Li, B., Matsumoto, M., Mizumori, S.J., Stephenson-Jones, M., and Vicentic, A. (2016). The Lateral Habenula Circuitry: Reward Processing and Cognitive Control. J. Neurosci. *36*, 11482–11488.

Borgius, L., Restrepo, C.E., Leao, R.N., Saleh, N., and Kiehn, O. (2010). A transgenic mouse line for molecular genetic analysis of excitatory glutamatergic neurons. Mol. Cell. Neurosci. *45*, 245–257.

Burstein, R., Cliffer, K.D., and Giesler, G.J., Jr. (1987). Direct somatosensory projections from the spinal cord to the hypothalamus and telencephalon. J. Neurosci. *7*, 4159–4164.

Duarte, J.O., Gomes, K.S., Nunes-de-Souza, R.L., and Crestani, C.C. (2017). Role of the lateral preoptic area in cardiovascular and neuroendocrine responses to acute restraint stress in rats. Physiol. Behav. *175*, 16–21.

Garland, J.C., and Mogenson, G.J. (1983). An electrophysiological study of convergence of entopeduncular and lateral preoptic inputs on lateral habenular neurons projecting to the midbrain. Brain Res. *263*, 33–41.

Heimer, L., and Alheid, G.F. (1991). Piecing together the puzzle of basal forebrain anatomy. In The Basal Forebrain, T.C. Napier, P.W. Kalivas, and I. Hanin, eds. (Springer), pp. 1–42.

Jhou, T.C., Good, C.H., Rowley, C.S., Xu, S.P., Wang, H., Burnham, N.W., Hoffman, A.F., Lupica, C.R., and Ikemoto, S. (2013). Cocaine drives aversive conditioning via delayed activation of dopamine-responsive habenular and midbrain pathways. J. Neurosci. *33*, 7501–7512.

Kawai, T., Yamada, H., Sato, N., Takada, M., and Matsumoto, M. (2015). Roles of the lateral habenula and anterior cingulate cortex in negative outcome monitoring and behavioral adjustment in nonhuman primates. Neuron *88*, 792–804.

Lecca, S., Meye, F.J., and Mameli, M. (2014). The lateral habenula in addiction and depression: an anatomical, synaptic and behavioral overview. Eur. J. Neurosci. *39*, 1170–1178.

Lerner, T.N., Shilyansky, C., Davidson, T.J., Evans, K.E., Beier, K.T., Zalocusky, K.A., Crow, A.K., Malenka, R.C., Luo, L., Tomer, R., and Deisseroth, K. (2015). Intact-brain analyses reveal distinct information carried by SNc dopamine subcircuits. Cell *162*, 635–647.

Li, B., Piriz, J., Mirrione, M., Chung, C., Proulx, C.D., Schulz, D., Henn, F., and Malinow, R. (2011). Synaptic potentiation onto habenula neurons in the learned helplessness model of depression. Nature *470*, 535–539.

Maroteaux, M., and Mameli, M. (2012). Cocaine evokes projection-specific synaptic plasticity of lateral habenula neurons. J. Neurosci. *32*, 12641–12646.

Matsumoto, M., and Hikosaka, O. (2007). Lateral habenula as a source of negative reward signals in dopamine neurons. Nature *447*, 1111–1115.

Meye, F.J., Lecca, S., Valentinova, K., and Mameli, M. (2013). Synaptic and cellular profile of neurons in the lateral habenula. Front. Hum. Neurosci. *7*, 860.

Meye, F.J., Soiza-Reilly, M., Smit, T., Diana, M.A., Schwarz, M.K., and Mameli, M. (2016). Shifted pallidal co-release of GABA and glutamate in habenula drives cocaine withdrawal and relapse. Nat. Neurosci. *19*, 1019–1024.

Mok, A.C., and Mogenson, G.J. (1972a). Effect of electrical stimulation of the septum and the lateral preoptic area on unit activity of the lateral habenular nucleus in the rat. Brain Res. *43*, 361–372.

Mok, A.C., and Mogenson, G.J. (1972b). An evoked potential study of the projections to the lateral habenular nucleus from the septum and the lateral preoptic area in the rat. Brain Res. *43*, 343–360.

Namboodiri, V.M.K., Rodriguez-Romaguera, J., and Stuber, G.D. (2016). The habenula. Curr. Biol. *26*, R873–R877.

Proulx, C.D., Hikosaka, O., and Malinow, R. (2014). Reward processing by the lateral habenula in normal and depressive behaviors. Nat. Neurosci. *17*, 1146–1152.

Root, D.H., Mejias-Aponte, C.A., Qi, J., and Morales, M. (2014a). Role of glutamatergic projections from ventral tegmental area to lateral habenula in aversive conditioning. J. Neurosci. *34*, 13906–13910.

Root, D.H., Mejias-Aponte, C.A., Zhang, S., Wang, H.L., Hoffman, A.F., Lupica, C.R., and Morales, M. (2014b). Single rodent mesohabenular axons release glutamate and GABA. Nat. Neurosci. *17*, 1543–1551.

Shabel, S.J., Proulx, C.D., Trias, A., Murphy, R.T., and Malinow, R. (2012). Input to the lateral habenula from the basal ganglia is excitatory, aversive, and suppressed by serotonin. Neuron *74*, 475–481.

Shabel, S.J., Proulx, C.D., Piriz, J., and Malinow, R. (2014). Mood regulation. GABA/glutamate co-release controls habenula output and is modified by antidepressant treatment. Science *345*, 1494–1498.

Stamatakis, A.M., Jennings, J.H., Ung, R.L., Blair, G.A., Weinberg, R.J., Neve, R.L., Boyce, F., Mattis, J., Ramakrishnan, C., Deisseroth, K., and Stuber, G.D. (2013). A unique population of ventral tegmental area neurons inhibits the lateral habenula to promote reward. Neuron *80*, 1039–1053.

Stamatakis, A.M., Van Swieten, M., Basiri, M.L., Blair, G.A., Kantak, P., and Stuber, G.D. (2016). Lateral hypothalamic area glutamatergic neurons and their projections to the lateral habenula regulate feeding and reward. J. Neurosci. *36*, 302–311.

Stephenson-Jones, M., Yu, K., Ahrens, S., Tucciarone, J.M., van Huijstee, A.N., Mejia, L.A., Penzo, M.A., Tai, L.-H., Wilbrecht, L., and Li, B. (2016). A basal ganglia circuit for evaluating action outcomes. Nature *539*, 289–293.

Stopper, C.M., and Floresco, S.B. (2014). What's better for me? Fundamental role for lateral habenula in promoting subjective decision biases. Nat. Neurosci. *17*, 33–35.

Yamaguchi, T., Sheen, W., and Morales, M. (2007). Glutamatergic neurons are present in the rat ventral tegmental area. Eur. J. Neurosci. *25*, 106–118.

Yamaguchi, T., Wang, H.L., Li, X., Ng, T.H., and Morales, M. (2011). Mesocorticolimbic glutamatergic pathway. J. Neurosci. *31*, 8476–8490.

Yang, L.-M., Hu, B., Xia, Y.-H., Zhang, B.-L., and Zhao, H. (2008). Lateral habenula lesions improve the behavioral response in depressed rats via increasing the serotonin level in dorsal raphe nucleus. Behav. Brain Res. *188*, 84–90.

Yetnikoff, L., Cheng, A.Y., Lavezzi, H.N., Parsley, K.P., and Zahm, D.S. (2015). Sources of input to the rostromedial tegmental nucleus, ventral tegmental area, and lateral habenula compared: a study in rat. J. Comp. Neurol. *523*, 2426–2456.

Zhang, S., Qi, J., Li, X., Wang, H.L., Britt, J.P., Hoffman, A.F., Bonci, A., Lupica, C.R., and Morales, M. (2015). Dopaminergic and glutamatergic microdomains in a subset of rodent mesoaccumbens axons. Nat. Neurosci. *18*, 386–392.